2018 IEEE-RAS 18th International Conference on Humanoid Robots (Humanoids)
Beijing, China, November 6-9, 2018

Fall Protection of Humanoids Inspired by Human Fall Motion

Wenpeng Ding[1], Xuechao Chen[1,2], Zhangguo Yu[1,2], Libo Meng[1,2], Marco Ceccarelli[1,3], Qiang Huang[1,2]

Abstract— **Most of the existing stability control methods for humanoids aim at avoiding falling down, and it is difficult to cope with the sudden fall of robots. However, humanoids is an unstable system which cannot avoid falling down. In this paper, we design a planning method of fall protection for humanoids according to the human fall motion. This method determines the contact position between the robot and the ground by adjusting the motion of the robot when it falls. In order to further reduce the damage to the robot, the appropriate cushioning material installed at the point of collision is selected to absorb the impact. The effectiveness of the proposed method is verified by BHR6P humanoid robot fall experiments.**

I. INTRODUCTION

The humanoids walk on both feet and have a smaller supporting area and a higher center of gravity than other types of robots. In addition, the humanoids generally have dozens of degrees of freedom; the structure is complex; the nonlinearity is high; and the control is difficult. This is one of the main bottlenecks restricting the application of humanoids. Since the DARPA Robotics Challenge, the fall of humanoids has received increasing attention and has become a research hotspot in the field of humanoids.

There are some limitations in the existing fall motion planning and control. A few of the methods that have been verified on large scale humanoids have their own shortcomings and are difficult to apply to motor-driven robots with large joint stiffness. Almost all of the rest only stay in the simulation verification or small humanoids verification phase.

Fujiwara et al. proposed a heuristic fall strategy and conducted a backward fall experiment through simulation and HRP-2 humanoid robot to verify the effectiveness of the proposed method [1], [2]. In the following research, Fujiwara et al. conducted the study of humanoid robot's fall protection movement through trajectory optimization, and verified the effectiveness of the algorithm on a simplified robotic fall platform [3], [4]. However, at the 2015 DARPA Robotics Challenge, the HRP-2 robot with fall protection was not able to stand up again after falling. For this reason, Kajita et al. proposed a method of using an inflatable backpack to protect the humanoids [5]. When the robot loses its balance, it can absorb most of the impact after a fall by quickly filling the air bag with CO_2 gas. However, this completely passive protection method is not versatile and it is difficult to adapt to different falls. Samy et al. make the arm have a certain flexibility when colliding with the ground by changing the PD parameters of the robot arm joints at the time of falling [6]. However, the joints of large-scale humanoids generally use harmonic reducers as transmission components and have a large reduction ratio. Even if the joint PD control parameters are reduced, the joint stiffness will still be relatively large. This way of the fall protection may cause greater damage to the robot arm joints. Ogata et al. proposed an optimized fall strategy to control the fall motion of the humanoids while walking [7]. In the subsequent study, they tested the fall method on the small robot platform HRP-2m Choromet to verify the effectiveness of the method. Yun et al. used the overall humanoids as a convex polygonal body to control the fall collision problem of the robot by controlling the shape of the polygonal body. The method was verified on the NAO small humanoid robot [8].

In this paper, the human fall experiments were carried out, and the law of human falling motion was obtained. A simplified model of the fall motion of the humanoids based on the third-order inverted pendulum was established as shown in Fig. 1, and made up for the inability of the linear inverted pendulum model to describe the rotation of the leg and trunk of the humanoids. According to the law of human fall [9] and the robot's own hardware, the constraints were given. Through the multi-stage optimization method of the nonlinear system, the fall motion trajectory that minimizes the impact was obtained. By comparing the performance of different materials, a suitable material was selected to absorb the impact. Finally, a control system and a fall protection device were designed for the BHR6P humanoid robot, and experiments were performed to verify the effectiveness of the proposed motion planning and control method of humanoids.

II. MOVEMENT ANALYSIS OF HUMAN FALL

Under normal circumstances, when people are standing normally, they can maintain their stability if they are not interfered or the external interference is relatively small. When the external disturbance gradually increases, the steady state changes. When the external disturbance exceeds the level that the human can resist, it will cause a fall. As shown in Fig. 2, the subject fell due to interference. The subject instinctively completed the action of lowering the center of gravity such as bending the knees and bending over. These actions can reduce the impact of collisions [10]. At the same time, these protective actions also determine the point of

This work was supported in part by the National Natural Science Foundation of China under Grant 61703043, 91748202, and 61533004, and in part by the 111 Project under Grant B08043.

[1]School of Mechantronical Engineering, Beijing Institute of Technology, Beijing 100081, China

[2]Beijing Advanced Innovation Center for Intelligent Robotics and Systems, Beijing Institute of Technology, Beijing 100081, China

[3]University of Cassino and South Latium, Italy.

Corresponding author: Xuechao Chen chenxuechao@bit.edu.cn

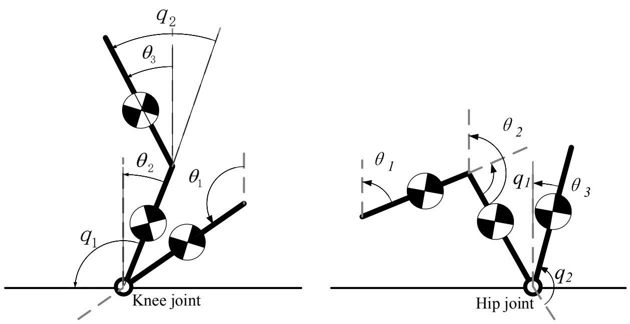

(a) Falling forward (b) Falling backward

Fig. 1. The model after falling down

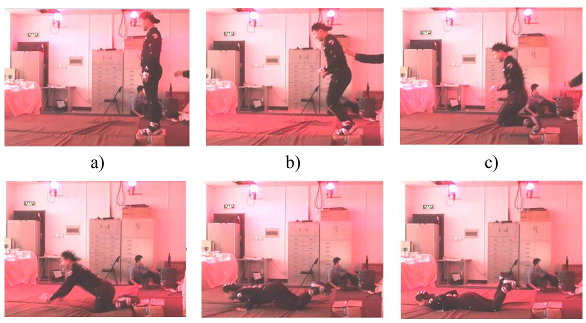

a) b) c) d) e) f)

Fig. 2. Falling experiment of human

contact between the human and the collision plane in the event of a collision. In most cases, the first point of collision that falls forward is the knee, then the arm or elbow. The main collision point that falls backward is the hip joint.

Through the analysis of the fall data of multiple groups of subjects, the body's posture remains between $-20°$ and $0°$ when the body falls forward, and the body posture remains between $0°$ and $25°$ when falling backward. Therefore, the body posture changes little during the air movement phase of the fall process, and basically maintains a vertical state. If the posture of the body changes too much, the angular momentum of the human in the sagittal plane will be too large, which makes it difficult for the human to adjust quickly after the collision, and may cause tumbling. Since the collision is unavoidable during the fall, an important purpose of the fall protection is to use the soft and elastic parts of the human to mitigate the impact of the collision. When falling forward, the knee is usually used as the first collision part to slow down the drop and complete the first level of buffer protection; The fall continues, and the subject's body begins to rotate along the knee. When the center of gravity is lowered to a certain height, the second level of cushioning of the fall is achieved by the hand touching the cushion and the muscle contraction of the arm. For a backward fall, the hip will be the first impact position. After absorbing the impact, the human uses the entire back as a second level buffer. The human uses a two-stage cushioning movement to minimize the impact of the fall and achieve a safe landing.

Through analysis, two major collisions occur when the human fall. According to the occurrence of the collision, the process of human fall is divided into four parts. Similar to the human fall, the fall of the humanoids can also be divided into four stages according to the occurrence of the collision: the stabilization and preparation phase, the air movement phase after the disturbance, the adjustment phase after the first collision, and the end of the fall after the second collision. According to the movement law of different stages of human fall, combined with the characteristics of humanoids structure, this paper designs a fall protection strategy:

- In the stage of air movement during the fall, try to keep the upper body posture close to the vertical direction to reduce the moment that the hip joint is subjected to during the first collision, and to avoid tumbling after the collision, causing secondary damage to the robot;
- Because this paper studies the sagittal fall, the robot should minimize the number of joints in motion during the air movement phase, and only use the hip joint and knee joint movement to lowered the center of gravity. The other joints of the legs remain stationary to avoid collision of the robot's leg structure, causing unnecessary damage to the robot.
- When the robot falls forward, the knee is used as the first collision point. When the robot falls backward, the hip is used as the first collision point. And a buffer device should be installed at the corresponding collision site to further absorb the impact of the collision. Usually the design guidelines for humanoids arms are lightweight and dexterous for gripping or other dexterous operations, and do not have similar impact resistance to human arms. Therefore, when the robot falls forward, try not to use the arm as a collision part.

III. FALL PROTECTION DEVICE

The buffer device is very important for the fall protection of the robot. We installed a fall protection device at the contact part between the robot and the ground to reduce the damage to the robot caused by the collision. By comparing the performance of different materials, combined with the requirements of the robot to fall on the material characteristics, the appropriate material was selected to buffer the fall of the robot.

The robot requires the buffer device to have a good buffering ability and does not rebound after touch. Although there are many types of cushions, they all have one drawback: To achieve good cushioning performance, mats are usually thicker. Although a variety of materials with different mechanical properties can be obtained by changing some processing techniques and material parameters, the cost is higher and the working hours are longer. By mixing various materials with different properties, materials with different properties can be more easily configured.

Although the honeycomb cushioning material is better than the foam cushioning material in the buffering effect, the honeycomb material is mostly applied to the unidirectional impact. In the impact of multiple directions, the cellular material has a ordinary buffering effect and poor processing performance, and is generally used for partial buffering. Although the buffering performance of the foam material in one direction is not as good as the honeycomb material, the buffering performance in all directions is better. On the whole, the foam material meets the robot fall requirements more than the honeycomb material. Therefore, this article focuses on several foam cushioning materials. Because the stacking order of materials is also related to the impact response, the material in figure is from left to right, and the stacking order is from top to bottom. For example, the A-B shock response in the figure indicates that the A material is at the top, the B material is at the bottom, and so on. Three kinds of materials were analyzed in the experiment: npgel, foamed silica gel (FSR), and sponge. Damping coefficient from the smallest to the largest: sponge $<$npgel $<$FSR.

Since the focus of this article is not on the dynamic impact response of the theoretical simulation, we only observed the dynamic impact response of different materials through experiments. The experiment is that the sole plate (1.045kg) is free to fall from a height of 0.82m. The cushioning material is placed on the force measuring table, the impact force is also measured on the force measuring table. After treatment with matlab, the response diagram of the impact acceleration and time is obtained. Fig. 3 is a impact response diagram of the free fall. Fig. 4 is a impact response diagram of a sponge as a cushion. Fig. 5-7 are impact comparison plots of three kinds of material aliasing: FSR-sponge-npgel vs FSR-npgel-sponge, sponge-FSR-npgel vs FSR-sponge-npgel, and sponge-npgel-FSR vs npgel- sponge-FSR. Because the stacking order has an influence on the mechanical properties of composite materials, there are 6 kinds of arrangement.

It can be found from Fig. 3-7:

- In the case of the same thickness, the sponge has the smallest impact force and the secondary impact force is also small. Although the sponge has a good cushioning effect, after the first contact with the ground was observed through the experimental, the height of object bouncing on the sponge was high, which could not meet the requirement of inelastic collision of the robot.
- In Fig. 7, keep the FSR at the bottom, swapping the position of the sponge and npgel. In the case where the impact force is almost constant, if the uppermost is a composite cushioning material with a large damping coefficient, the secondary impact force is small. Observed by experimental, the height of the bounce is lower after the first touchdown. The above conclusions can also be drawn from the comparison of Fig. 6.

In summary, the robot adopts the FSR-npgel-sponge composite buffer material to ensure that the impact force is small and the robot does not bounce after the first collision, thereby satisfying the conditions for the trajectory algorithm.

IV. MATHEMATICAL MODEL

Humanoids is a complex nonlinear system with multi degree of freedom. The whole-body dynamics solving for humanoids is cumbersome and computationally intensive, and

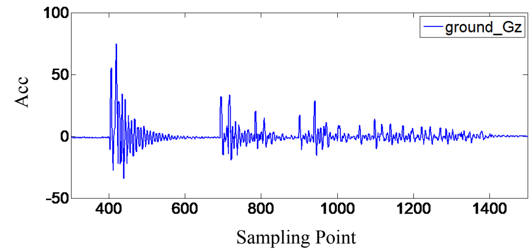

Fig. 3. Response diagram with unbuffered collision

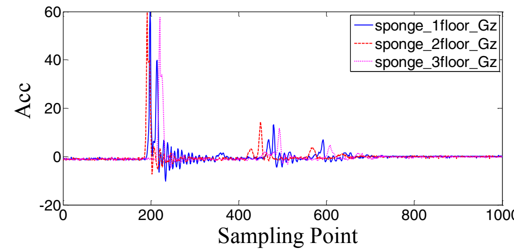

Fig. 4. Response diagram with sponge collision

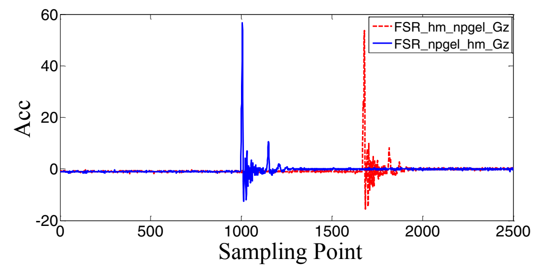

Fig. 5. Comparison of FSR-sponge-npgel vs FSR-npgel-sponge buffering capabilities

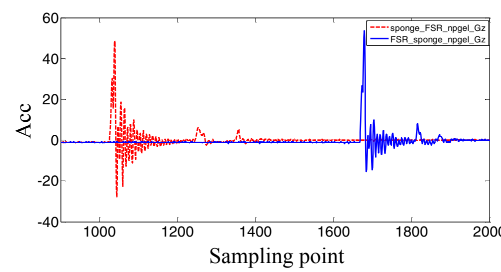

Fig. 6. Comparison of sponge-FSR-npgel vs FSR-sponge- npgel buffering capabilities

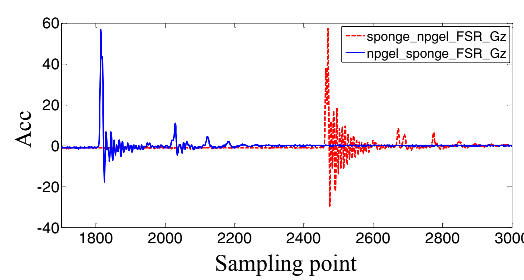

Fig. 7. Comparison of sponge-npgel-FSR vs npgel-sponge-FSR buffering capabilities

it is difficult to satisfy the robot online planning and control. Therefore, when performing humanoids motion planning, most researchers use robot simplified models for trajectory calculation and real-time adjustment. In this paper, the third-order inverted pendulum model is used as a simplified model, and the motion planning of the robot's fall is performed accordingly.

A. Dynamic Model

The collision as a node can divide the falling of the humanoids into two phases: the first phase is the movement phase from the standing state to the first collision; and the second phase is the period from the first collision to the second collision. Each fall motion of the robot can be simplified as a third-order inverted pendulum movement with different fulcrums.

As shown in Fig. 1, the first-stage link is from the edge along the foot to the knee joint, with a length of L_1 and a mass of M_1. The angle between the connecting rod and the vertical direction is θ_1, the length of the centroid from the lower end of the connecting rod is l_1, and the inertia with respect to the center of mass is I_1. The second-stage link and the third-stage link are similar to the first-stage link. The model has two active degrees of freedom, namely the movement q_1 of the knee joint and the movement q_2 of the hip joint, and a passive degree of freedom that rotates around the ground.

The dynamic equation of robot is the description of the robot motion state, and is the basis for the motion planning and control. In this paper, the Lagrange equation [11] is used to solve the dynamic equation of the third-order inverted pendulum model.

$$\mathbf{L}(\theta,\dot{\theta}) = \mathbf{K}(\theta,\dot{\theta}) - \mathbf{V}(\theta) \tag{1}$$

$$\frac{d}{dt}\frac{\partial \mathbf{L}}{\partial \dot{\theta}} - \frac{\partial \mathbf{L}}{\partial \theta} = \Gamma \tag{2}$$

The generalized force Γ of the system is as follow:

$$\Gamma = \mathbf{B}(\theta)\mathbf{u} \tag{3}$$

The dynamic model of the robot can be described by the Lagrange dynamics equation as follow:

$$\mathbf{D}(\theta)\ddot{\theta} + \mathbf{C}(\theta,\dot{\theta}) + \mathbf{G}(\theta) = \mathbf{B}(\theta)\mathbf{u} \tag{4}$$

Where $\mathbf{D}(\mathbf{q})$ is the inertia matrix of each member, $\mathbf{G}(\mathbf{q})$ is the gravity term, and $\mathbf{C}(\mathbf{q},\dot{\mathbf{q}})$ is the resultant vector of Coriolis force and centrifugal force. For the first-stage fall motion of the humanoids, the end of the three-link is in contact with the ground and is in a free-motion state. The ground has no torque input to the robot, so τ is only the input torque of the knee joint and the hip joint. Matrix B is a mapping matrix that maps joint input torque to generalized forces. For humanoids simplified to three-link, u is the input torque $[\tau_1 \;\; \tau_2]^T$ of the knee joint and hip joint. Because the ground has no torque input to the robot, the rotation angle of the knee joint and the hip joint is the relative angle between the driving joints. So matrix B can be calculated by formula 5 and formula 6:

$$\mathbf{B}(\theta) = \left(\frac{\partial}{\partial \theta}\begin{bmatrix} q_1 \\ q_2 \end{bmatrix}\right)' \tag{5}$$

$$\begin{cases} q_1 = -\theta_1 + \theta_2 \\ q_2 = -\theta_2 + \theta_3 \end{cases} \tag{6}$$

Therefore, the parameters of $\mathbf{D}(\theta)$, $\mathbf{C}(\theta,\dot{\theta})$, $\mathbf{G}(\theta)$ can be solved according to formula 1-6.

In the second stage of fall, the coefficient matrix $B(\theta)$ on the right side of formula 1 does not change. Due to the change of the action point between the robot and the ground, the configuration of the second stage of the robot falling down is different from that of the first stage. Therefore, the calculation formula for the potential energy and kinetic energy of the robot is different, which causes the inertia matrix, the Coriolis force matrix, and the gravity matrix on the left side of the equation to change and needs to be recalculated. The method of calculating the coefficient matrix is the same as that of the first stage of the fall and we do not state any more. In summary, the first collision of the robot falling as a node can describe the robot's fall process as follows:

$$\begin{cases} D_s(\theta)\ddot{\theta} + C_s(\theta,\dot{\theta}) + G_s(\theta) = B(\theta)u, Phase1 \\ D_f(\theta)\ddot{\theta} + C_f(\theta,\dot{\theta}) + G_f(\theta) = B(\theta)u, Phase2 \\ D_b(\theta)\ddot{\theta} + C_b(\theta,\dot{\theta}) + G_b(\theta) = B(\theta)u, Phase2 \end{cases} \tag{7}$$

Where $D_s(\theta)$, $C_s(\theta,\dot{\theta})$, $G_s(\theta)$ are the coefficient matrix when the robot stands and falls in the first stage; $D_f(\theta)$, $C_f(\theta,\dot{\theta})$, $G_f(\theta)$ are the coefficient matrix when the robot falls forward in the second stage and $D_b(\theta)$, $C_b(\theta,\dot{\theta})$, $G_b(\theta)$ are the coefficient matrix when the robot falls backward in the second stage.

The main reason that the humanoids is injured in a fall is a fierce collision with the ground. The huge impact caused by the collision will destroy the mechanical structure of the robot or cause the electrical components to fail, resulting in the robot can not continue to work. Therefore, how to reduce the impact of collision is the key to the fall protection of the humanoids. This paper establishes the relationship between the movement state of the humanoids and the collision when it falls, so that the collision impact can be controlled by controlling the falling motion of the robot. When the robot collides with the ground:

$$D(\theta)\ddot{\theta} + C(\theta,\dot{\theta}) + G(\theta) = B(\theta)u + B'\delta F \tag{8}$$

Where $\delta F = (\delta F_T, \delta F_N)$ is the impact force acting on the collision point $p = (p_h; p_v)$, and B' transforms the collision force F into the transformation coordinates of the generalized force:

$$B' = \left(\frac{\partial}{\partial p}\begin{bmatrix} q_1 \\ q_2 \end{bmatrix}\right)' \tag{9}$$

Suppose that the collision occurs at time t and the collision time is very short. We can get integral from both ends of formula 8:

$$\int_{t^-}^{t^+}(D(\theta)\ddot{\theta}+C(\theta,\dot{\theta})+G(\theta))dt=\int_{t^-}^{t^+}(B(\theta)u+B'\delta F)dt \tag{10}$$

Assuming that the collision between the robot and the ground is a completely inelastic collision, the collision will only change the speed of the robot and cannot change the configuration of the robot immediately. Therefore, the angles θ^+ and θ^- of each link in the world coordinate system do not change before and after collision, that is:

$$\theta^+=\theta^- \tag{11}$$

Formula 10 can be changed to:

$$D(\theta^+)\dot{\theta}^+-D(\theta^-)\dot{\theta}^-=B^{'}F \tag{12}$$

Next, we study the collision between the robot and the ground based on the collision of the knee with the ground when the robot falls down. When the knee lands in a completely inelastic collision, the velocity changes to zero immediately. The relationship between the velocity of the knee and the angular velocity $\dot{\theta}$ of the bar can be expressed by Jacobi matrix:

$$J_{knee}(\theta^-)\dot{\theta}^-=v_{knee}^- \tag{13}$$

$$J_{knee}(\theta^+)\dot{\theta}^+=0 \tag{14}$$

According to formula 11-14, the momentum change during collision can be obtained as follow:

$$F=-B^{'-1}J_{knee}^{-1}(\theta)D(\theta)J_{knee}(\theta)\dot{\theta}^- \tag{15}$$

The upper equation is the relationship between the robot motion state and the collision impact, so the size of the collision impact can be adjusted by controlling the state θ and $\dot{\theta}$ of the humanoid robot at the collision time t.

B. The Motion Planning of the Humanoids Fall Protection

The purpose of the humanoid robot's fall protection movement is to reduce the impact by the robot's own movement. Due to the hardware constraints, such as motor power, range of motion of the joint, etc, the movement of the robot is limited. Therefore, the motion planning of the humanoid robot's fall protection can be converted to the optimization problem with given constraints and optimization indexes.

Taking the first collision as the dividing point, the fall of the humanoids can be divided into two stages. The second stage of the process is divided into two cases according to the fall direction, and different stages are defined by the parameter p. Each movement can be described by the dynamic equation, and the dynamic equation can be regarded as a dynamic system. Therefore, the multi-stage optimization method of the nonlinear system can be used to obtain the trajectory of the robot's fall, making the impact minimum under the given constraints [12]-[16]. According to the formula 4, the joint torque τ is used as the input $\mathbf{u}$; the joint angle and angular velocity are used as the state variable $\mathbf{x}$, and the state equation of the fall motion of the humanoids can be established.

$$\dot{\mathbf{x}}=\mathbf{f}(\mathbf{x},\mathbf{u}) \tag{16}$$

$$\mathbf{x}:=\begin{bmatrix}\theta\\ \dot{\theta}\end{bmatrix} \tag{17}$$

The first stage of falling down (p=1)

$$\mathbf{f}(\mathbf{x},\mathbf{u}):=\begin{bmatrix}\dot{\theta}\\ \mathbf{M_s^{-1}}(\theta)(\mathbf{B_s}\mathbf{u}-\mathbf{C_s}(\theta,\dot{\theta})-\mathbf{G_s}(\theta))\end{bmatrix} \tag{18}$$

Falling forward in the second stage (p=2)

$$\mathbf{f}(\mathbf{x},\mathbf{u}):=\begin{bmatrix}\dot{\theta}\\ \mathbf{M_f^{-1}}(\theta)(\mathbf{B_f}\mathbf{u}-\mathbf{C_f}(\theta,\dot{\theta})-\mathbf{G_f}(\theta))\end{bmatrix} \tag{19}$$

Falling backward in the third stage (p=3)

$$\mathbf{f}(\mathbf{x},\mathbf{u}):=\begin{bmatrix}\dot{\theta}\\ \mathbf{M_b^{-1}}(\theta)(\mathbf{B_b}\mathbf{u}-\mathbf{C_b}(\theta,\dot{\theta})-\mathbf{G_b}(\theta))\end{bmatrix} \tag{20}$$

After the multi-stage equation of state is established, the optimization of the desired trajectory is changed into the establishment of constraints and cost functions. And under the given segmented state equations and various constraints, the cost function gets the lowest value.

In the first phase of the fall, to keep the robot as close as possible to the vertical state (determined by the angle θ) during the fall, the robot's body posture when falling forward is satisfied:

$$\theta_3^{'}<\theta_3<0^\circ \tag{21}$$

Let t be the time when a robot collides. When the robot falls forward, it should ensure that the knee collides with the ground firstly:

$$\theta_1(t)=90^\circ \tag{22}$$

When the robot falls backward:

$$0^\circ<\theta_3<\theta_3{''} \tag{23}$$

It should ensure that the hip joint collides with the ground firstly.

$$\theta_3(t)<90^\circ \tag{24}$$

According to the law of human fall movement of different age groups and the actual situation of the robot, the range of $\theta_3^{'}$ is $-20^\circ\sim-30^\circ$, and the range of $\theta_3{''}$ is $30^\circ\sim40^\circ$. This paper takes the average of -25° and 35° as the angle of the joint when the robot falls.

When performing humanoids fall planning, the hardware condition constraints of the robot should be considered, including the restriction of the robot's joint, the moving parts of the robot do not interfere with each other, the restriction of the output speed $\mathbf{n}$ of the joint and the output torque $\tau_{\mathbf{peak}}(\mathbf{n})$ at the current speed. The reduction ratios of knee joint and hip joint are i_{knee} and i_{hip} respectively, and the transmission efficiency are η_{knee} and η_{hip} respectively. Therefore, the constraints of joint movement when falling are:

$$\begin{cases} \mathbf{q_{min}} < \mathbf{q} < \mathbf{q_{max}} \\ |\dot{\mathbf{q}}| < \dot{\mathbf{q}}_{\mathbf{max}} \\ |\tau| < \mathbf{i} \circ \eta \circ \tau_{\mathbf{peak}}(\mathbf{n}) \end{cases} \tag{25}$$

Where $\mathbf{q_{min}}$ and $\mathbf{q_{max}}$ are the joint limit of the robot, $\mathbf{i} = [\mathbf{i_{knee}} \ \mathbf{i_{hip}}]^{\mathbf{T}}, \eta = [\eta_{\mathbf{knee}} \ \eta_{\mathbf{hip}}]^{\mathbf{T}}$. $\circ$ is operator of fractional prime product, which means matrix multiplication of corresponding elements [17].

The ultimate purpose of fall protection is to reduce the impact and to protect the robot. Based on the above reasons, the cost function is established:

$$E = \sum_{p=1}^{2} J^{(p)} \tag{26}$$

$J^{(p)}$ is the cost function at the corresponding stage of fall motion. In the first stage of the fall (p=1), it is hoped that the robot will receive as little impact as possible during the collision. Therefore, the cost function at this stage can be established as:

$$J^{(1)} = \begin{cases} (B'^{-1}J_{knee}^{-1}(q(t_i))D(q(t_i))\dot{q}^{-})^2 & Forward \\ (B'^{-1}J_{hip}^{-1}(q(t_i))D(q(t_i))\dot{q}^{-})^2 & Backward \end{cases} \tag{27}$$

In the second stage after the collision, the robot will make a free turn around the knee or hip joint, hoping that the impact of the second collision is as little as possible. In order to ensure the stability of the robot's final contact with the ground, the angular momentum after impact should be minimized. So the cost function can be obtained as follows:

$$\begin{aligned} J^{(2,3)} = K_1(\sum_{i=1}^{3}(M_i r_i \times v_i + I_i \omega_i))^2 + \\ K_2(B'^{-1}J_{hip}^{-1}(\theta(t_i))D(\theta(t_i))\dot{\theta}^{-})^2 \end{aligned} \tag{28}$$

The first term on the right side of the expression is the angular momentum of the robot, and the second term is the impact on the second collision. K_1 and K_2 are proportional coefficients that are used to adjust the weights of the cost functions.

This paper establishes a multi-stage state equation of the fall for the humanoids, and the corresponding constraints and cost functions for each phase. The optimal robotic fall motion trajectory can be obtained through a multi-stage optimization method of a nonlinear system.

V. EXPERIMENTAL VERIFICATION

This section will verify the proposed planning method through experimentation. The robot used in this article is the BHR6P humanoid robot. The fall protection device and the compact control electrical system are designed to improve the anti-drop capability of the entire system. The BHR6P humanoid robot has 21 degrees of freedom, a body weight of 60kg, and a height of 1.7m, as shown in Fig. 8.

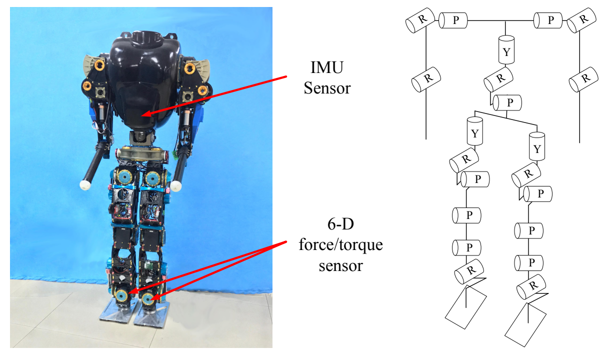

Fig. 8. BHR6P humanoid robot and its freedom configuration

During the robotic fall test, the current state of the robot is acquired through a six-dimensional force/torque sensor mounted on the sole of the foot and an IMU sensor installed in the chest cavity. Fig. 9 is a video capture of the robot's forward fall experiment.

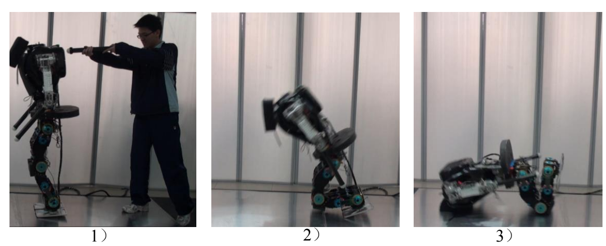

Fig. 9. Forward fall experiment of BHR6P humanoid robot

Fig. 10 shows the change in acceleration of the robot during the forward fall as recorded by the IMU sensor. It can be seen from the figure that the maximum value of acceleration occurs when the knee and chest collide with the ground, and the maximum values are about 6G and 15G respectively. In general, most of the hardware of the humanoids can withstand the acceleration of 20-30G [5], so the experimental results can verify the effectiveness of the forward fall protection motion proposed in this paper. Fig. 11 is a video capture of the robot's backward fall experiment.

Fig. 12 shows the change in acceleration of the robot during the backward fall as recorded by the IMU sensor. Acceleration of both collisions is within 20G, and it is possible to ensure that the hardware of the humanoids is not damaged.

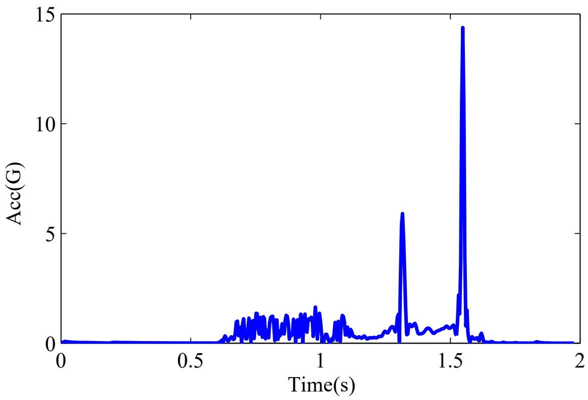

Fig. 10. Experimental results of forward fall of BHR6P humanoid robot

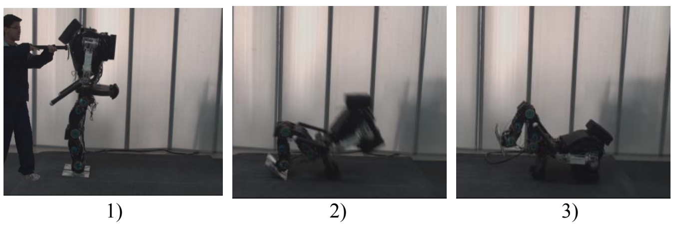

Fig. 11. Backward fall experiment of BHR6P humanoid robot

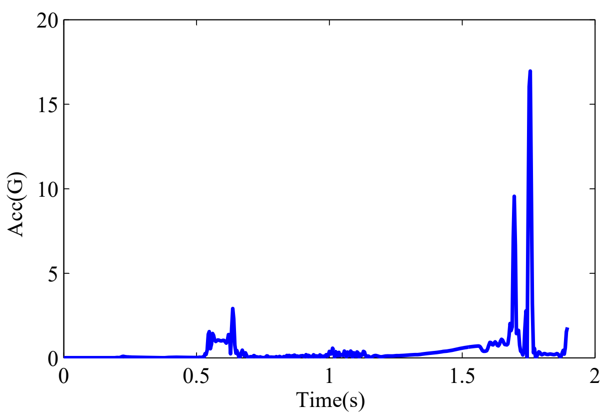

Fig. 12. Experimental results of backward fall of BHR6P humanoid robot

VI. CONCLUSIONS

In this paper, we have described our proposed method of falling protection for humanoids. Our method has the following major contributions.

(1). Based on the principle of bionics, the human fall motion test was carried out, and the body fall motion data was obtained. By analyzing the fall data, the movement law of human body fall is obtained, and the humanoids fall motion strategy is proposed.

(2). With the joint angle of the robot as the state variable and the joint input torque as the input, the humanoids fall motion equation is established. Combined with the law of human fall and the hardware constraints of humanoids, the optimization method is proposed, and the robot fall motion track which minimizes the impact of collision is obtained.

(3). Comparing the material properties of different cushioning materials, the appropriate material stacking sequence was chosen to absorb the impact.

(4). Finally, the effectiveness of the proposed fall protection method is verified by experiments on the BHR6P humanoid robot platform.

REFERENCES

[1] K. Fujiwara, F. Kanehiro, S. Kajita, et al. UKEMI: Falling motion control to minimize damage to biped humanoid robot. In IEEE/RSJ international conference on Intelligent robots and systems,2002: 2521-2526.

[2] K. Fujiwara, F. Kanehiro, S. Kajita, et al. The first human-size humanoid that can fall over safely and stand-up again. In IEEE/RSJ International Conference on Intelligent Robots and Systems,2003: 1920-1926.

[3] K. Fujiwara, S. Kajita, K. Harada, et al. Towards an optimal falling motion for a humanoid robot.In IEEE-RAS International Conference on Humanoid Robots,2006: 524-529.

[4] K. Fujiwara, S. Kajita, K. Harada, et al. An optimal planning of falling motions of a humanoid robot. In IEEE/RSJ International Conference on Intelligent Robots and Systems, 2007: 456-462.

[5] S. Kajita, R. Cisneros, M. Benallegue, et al. Impact acceleration of falling humanoid robot with an airbag. In IEEE-RAS International Conference on Humanoid Robots, 2016: 637-643.

[6] V. Samy, A. Kheddar. Falls control using posture reshaping and active compliance. In IEEE-RAS International Conference on Humanoid Robots, 2015: 908-913.

[7] K. Ogata, K. Terada, Y. Kuniyoshi. Falling motion control for humanoid robots while walking.In IEEE-RAS International Conference on Humanoid Robots, 2007: 306-311.

[8] S. Yun, A. Goswami. Tripod fall: Concept and experiments of a novel approach to humanoid robot fall damage reduction. In IEEE International Conference on Robotics and Automation, 2014:2799-2805.

[9] L. Meng, M. Ceccarelli, Z. Yu, X. Chen and Q. Huang. An Experimental Characterization of Human Falling Down, Mechanical Sciences, 8(1),pp. 79-89, 2017.

[10] S. N. Robinovitch, R. Brumer, J. Maurer. Effect of thesquat protective responseon impact velocity during backward falls [J]. Journal of biomechanics, 2004, 37 (9): 1329C1337.

[11] E. R. Westervelt, C. Chevallereau, J. H. Choi, et al. Feedback control of dynamic bipedal robot locomotion. CRC press, 2007.

[12] A. V. Rao, D. A. Benson, C. Darby, et al. Algorithm 902: Gpops, a matlab software for solving multiple-phase optimal control problems using the gauss pseudospectral method. ACM Transactions on Mathematical Software (TOMS), 2010, 37 (2): 22.

[13] D. A. Benson, G. T. Huntington, T. P. Thorvaldsen, et al. Direct trajectory optimization and costate estimation via an orthogonal collocation method. Journal of Guidance, Control, and Dynamics, 2006, 29 (6): 1435-1440.

[14] D. Garg, M. A. Patterson, C. Francolin, et al. Direct trajectory optimization and costate estimation of finite-horizon and infinite-horizon optimal control problems using a Radau pseudospectral method. Computational Optimization and Applications, 2011, 49 (2): 335-358.

[15] D. Garg, M. Patterson, W. W. Hager, et al. A unified framework for the numerical solution of optimal control problems using pseudospectral methods. Automatica, 2010, 46 (11): 1843-1851.

[16] D. Garg, W. W. Hager, A. V. Rao. Pseudospectral methods for solving infinite-horizon optimal control problems. Automatica, 2011, 47 (4): 829-837.

[17] C. Davis. The norm of the Schur product operation. Numerische Mathematik, 1962, 4 (1): 343-344.